tables of positional and thermal parameters, bond distances and angles, and hydrogen atom positional and thermal parameters, and information concerning diffraction experiments with twinned crystals of $AgOTeF_5(CH_2Cl_2)$ (10 pages); table of observed and calculated structure factors (16 pages). Ordering information is given on any current masthead page.

The Al(^{2}P){SiH_4} Complex and the Photoreversible Oxidative-Addition/Reductive-Elimination Reaction: Al(^{2}P){SiH_4} ⇄ H_3SiAlH

Michael A. Lefcourt and Geoffrey A. Ozin*

Lash Miller Chemistry Laboratory
University of Toronto, 80 St. George Street
Toronto, Ontario, Canada M5S 1A1

Received April 22, 1988

Weakly bound complexes between CH_4 and metal atoms in their *ground electronic states* (GS) have proven to be difficult species to detect and characterize by either gas-phase or matrix-isolation techniques.[1] One would anticipate that the longer, weaker SiH bonds of SiH_4 and the existence of low-lying empty 3d-orbitals would open up favorable electronic/structural channels for enhanced interactions with GS metal atoms compared to its lighter congener CH_4. In this communication we report spectroscopic and ab initio quantum chemical details for the Al(^{2}P){SiH_4} complex which support this view as well as information on the photoreversible oxidative-addition/reductive-elimination reaction:

$$Al(^2P)\{SiH_4\} \rightleftarrows H_3SiAlH$$

On depositing Al atoms into progressively doped SiH_4/Ar mixtures at 12 K, passing from neat Ar to neat SiH_4, one notes in the optical spectrum a smooth transformation from narrow Al atom $^2S \leftarrow {}^2P$ (340 nm), $^2D \leftarrow {}^2P$ (293, 288, 280 nm) excitations to a situation displaying broad, structured absorptions around 450–350 and 280–245 nm (Figure 1A–D). The substitution of SiH_4 for SiD_4 caused significant narrowing of these two broad features on the order of ~475 and ~150 cm^{-1} for the low- and high-energy absorptions, respectively (silane:argon = 1:10, Figure 1C), implicating a silane complex as the species responsible for the Al/SiH_4 optical spectrum.

The corresponding EPR spectra of Al/SiH_4 and Al/SiD_4 strongly support this view. In brief, the axial Al(^{2}P) hyperfine sextet observed in solid Ar at 12 K (^{27}Al, $I = {}^5/_2$, natural abundance 100%, Figure 2A) on progressively doping with increased concentrations of SiH_4, is replaced by the dramatically distinct EPR spectra depicted in Figure 2 (parts B, C-i, and D). Since the differences exhibited within this group are very small relative to the change observed upon initial doping (silane:argon = 1:100, Figure 2 (parts A to B)), it is reasonable to postulate a 1:1 stoichiometry for the proposed Al(^{2}P){SiH_4} complex assuming that a statistical dispersion of the SiH_4 in Ar exists upon matrix formation. The participation of SiH_4 in the species responsible for these EPR spectra is demonstrated by the narrowing of the observed Al hyperfine lines in Al/SiD_4 matrices; $\beta_N^D/\beta_N^H = 0.307$ (Figure 2C-ii) consistent with the optical results described above.

In concert with the EPR spectral diagnostics, spin Hamiltonians including axial and orthorhombic magnetogyric tensors, ^{27}Al hyperfine and ^{1}H/^{2}H superhyperfine tensors, were employed to computer-model the EPR transitions of the different C_{3v}, C_{2v}, and C_s Al(^{2}P){SiH_4} geometries in attempts to simulate the experimental spectra. Excellent best-fit simulations[2] (omitting contributions from paramagnetic ^{29}Si; $I = {}^1/_2$, natural abundance 4.7%) could be obtained for each of these Al{SiH_4} interaction schemes (i.e., Figure 2C-i) including in the spectra the presence of superimposed trace amounts of isolated SiH_3 radicals: $g_\parallel = 2.004$, $g_\perp = 2.006$, $A_\parallel = 17$ MHz, and $A_\perp = 23$ MHz (cf. ref 3). Preliminary ab initio quantum chemical calculations[4] favor the C_s geometry similar to the three-center

bonding schemes in known hydrosilyl complexes of certain Cr- and Mn-containing organometallic compounds determined by

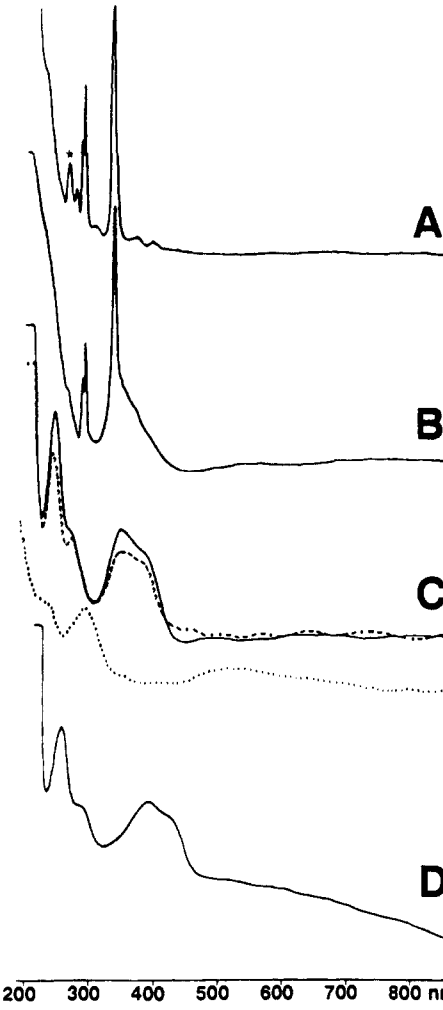

Figure 1. UV–vis spectra (12 K, ~6 μg total metal; ~1:10^4 dilution in host). * indicates band due to Al_2: (A) Al/Ar deposition spectrum. (B) Al/(1:100 SiH_4/Ar) deposition spectrum. (C) (—) Al/(1:10 SiH_4/Ar) deposition spectrum, (– – –) Al/(1:10 SiD_4/Ar) deposition spectrum, (···) Al/(1:10 SiH_4/Ar) after photolysis at 400 nm (20 nm fwhm) for 11 min. (D) Al/SiH_4 deposition spectrum.

(1) (a) Ozin, G. A. *Methane Activation on Single Metal Atom Sites*; Gas Research Institute Methane Activation Conference Proceedings, Houston, TX, 1985. (b) Trammel, G. T.; Zeldes, H.; Livingston, R. *Phys. Rev.* **1958**, *110(3)*, 630. (c) Bowman, M.; Kevan, L. *Chem. Phys. Lett.* **1975**, *30(2)*, 208.

(2) Fitting programs written by Lozos, G.; Hoffman, B.; Franz, C. Department of Chemistry, Northwestern University, Evanston, IL. Versions of these programs exist at the Department of Chemistry, University of Toronto, Toronto, Ontario, Canada.

(3) (a) Raghunathan, P.; Shimokoshi, K. *Spectrochim. Acta* **1980**, *36A*, 285. (b) Morehouse, R. L.; Christiansen, J. J.; Gordy, W. *J. Chem. Phys.* **1966**, *45*, 1751.

(4) (a) MONSTERGAUSS software package written by: Peterson, M. R. Department of Chemistry, University of Toronto, Toronto, Canada, and Poirier, R. A. Department of Chemistry, Memorial University, St. John's, Newfoundland, Canada. (b) 3-21G split-valence basis-set: Binkley, J. S.; Pople, J. A.; Hehre, W. J. *J. Am. Chem. Soc.* **1980**, *102*, 939. (c) Spin-restricted Hartree–Fock method: Kato, S.; Morokuma, K. *Chem. Phys. Lett.* **1979**, *65*, 19. An extensively modified version was adapted for MONSTERGAUSS. (d) Geometry optimizations, optimally-conditioned gradient method: Davidon, W. C.; Nazareth, L. Argonne National Laboratories Technical Memos 303 and 306, Argonne, IL.

0002-7863/88/1510-6888$01.50/0

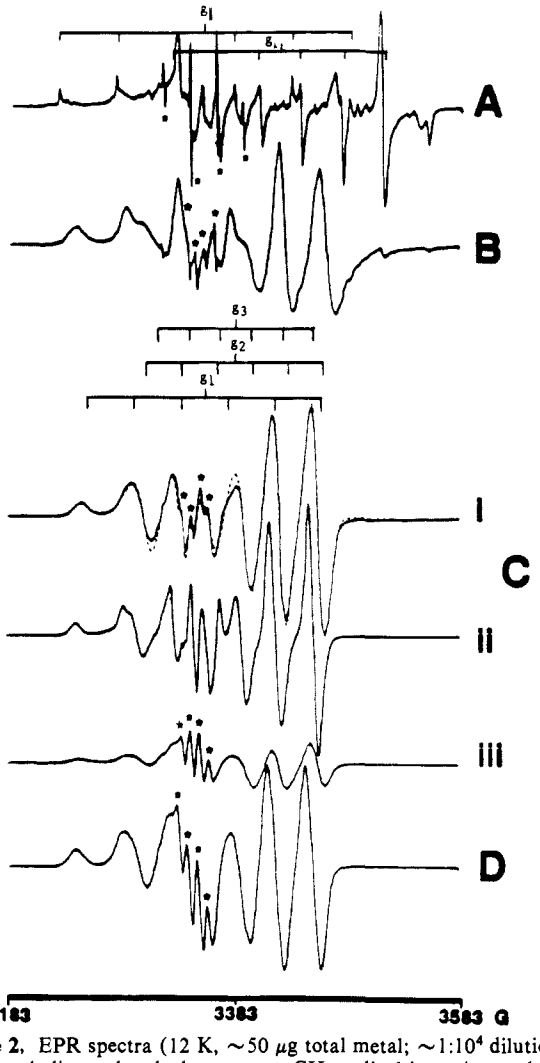

Figure 2. EPR spectra (12 K, ~50 μg total metal; ~1:10⁴ dilution in host). ■ indicates bands due to trace CH_3 radical impurity, and * indicates bands due to trace SiH_3 radical: A. Al/Ar deposition spectrum; $g_{\parallel}$, $g_{\perp}$, and Al hyperfine splittings shown as stick spectra are qualitative. B. Al/(1:100 SiH_4/Ar) deposition spectrum. C.i. (—) Al/(1:10 SiH_4/Ar) deposition spectrum; (---) computer simulation for Al(^{2}P){SiH_4} employing the C_s model 1-proton orthorhombic interaction. RMS = 0.030. g values and Al hyperfine splittings are shown as qualitative stick spectra (see text for best-fit parameters). ii. Al/(1:10 SiD_4/Ar) deposition spectrum. iii. Al/(1:10 SiH_4/Ar) after photolysis at 400 nm (20 nm fwhm) for 90 min. D. Al/SiH_4 deposition spectrum.

XRD.[5] On these grounds we report the results of the excellent orthorhombic fit obtained for this model of the Al(^{2}P){SiH_4} complex: $g_1 = 1.999$, $g_2 \simeq g_3 = 1.982$; A_1(Al) = 117, A_2(Al) = 88, A_3(Al) = 77 MHz; A_1(H) = 13, A_2(H) = 18, A_3(H) = 16 MHz, as well as the calculated atomic spin-densities:[6] ρ_{Al}(3p) = 80.1, ρ_{Al}(3s) = 0.4, ρ_H(1s) = 1.1% (cf. Al/CH_4:[7] ρ_{Al}(3p) = 93.2, ρ_{Al}(3s) = 0.5%; Al/Ar:[8] ρ_{Al}(3p) = 98.3, ρ_{Al}(3s) = 0.5%). A dramatic decrease in the Al atom 3p spin-density is observed on passing from Al/Ar to Al/SiH_4, approximately 3.5 × larger than the effect from Al/Ar to Al/CH_4. In Al(^{2}P){SiH_4} only ~82% of the unpaired spin-density can be accounted for by the Al(3s/3p) and the H(1s), implying that most of the remaining ~18% is residing on the silicon. It should be stressed however that these values are approximate due to the method of their determination.[6]

Additional support for the identification of the GS Al(^{2}P){SiH_4} complex stems from its photochemical conversion to the insertion product H_3SiAlH. This transformation ($h\nu$ = 400 nm, fwhm = 20 nm),[9] is clearly seen by the loss of Al(^{2}P){SiH_4} optical and

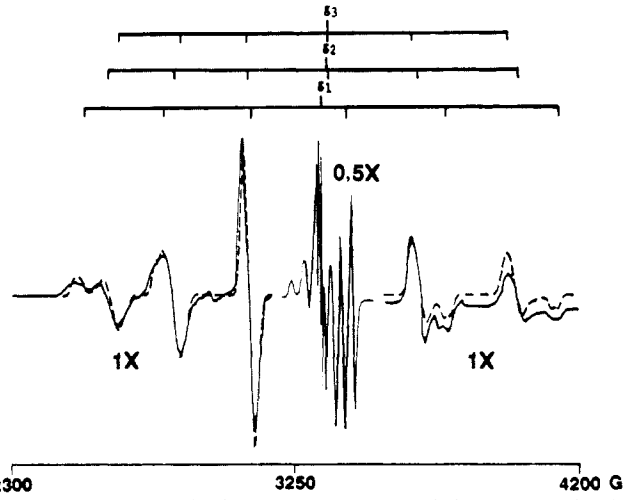

Figure 3. Expanded field EPR spectrum recorded at increased gain showing photolysis product resonances. Separated central region absorptions are due to unreacted Al(^{2}P){SiH_4} and correspond to the spectrum shown in Figure 2C-iii. (—) Al/(1:10 SiH_4/Ar) after photolysis at 400 nm (20 nm fwhm) for 90 min. (---) computer simulation for nonlinear H_3SiAlH (orthorhombic, C_s symmetry) RMS = 0.067. g values and Al hyperfine splittings are shown as qualitative stick spectra (see text for best-fit parameters).

EPR spectral signatures and their replacement by product absorptions (Figures 1C, 2C-iii, and 3), together with the concomitant evolution of IR absorptions at 2116, 1784, and 842 cm^{-1}, which show identical growth patterns and characteristic isotope shifts to 1522, 1300, and 628 cm^{-1}, on substituting SiH_4 for SiD_4. Of particular note is the striking similarity of some of the EPR/IR/optical properties of the Al(^{2}P){SiH_4} photoproduct to those recently reported for H_3CAlH.[7,10] The EPR spectra for both molecules correspond to orthorhombic species displaying single Al atom hyperfine and single hydrogen superhyperfine splittings: $g_1 = 2.006$, $g_2 = 2.003$, $g_3 = 2.002$; A_1(Al) = 890, A_2(Al) = 753, A_3(Al) = 717 MHz; A_1(H) ≃ A_2(H) ≃ A_3(H) = 62 MHz for H_3SiAlH, and $g_1 \simeq g_2 = 2.002$, $g_3 = 2.000$; A_1(Al) = 880, A_2(Al) = 723, A_3(Al) = 712 MHz; A_1(H) = 157, A_2(H) = 146, A_3(H) = 154 MHz for H_3CAlH.[11] High level ab initio calculations (6-31G**)[12] yield bond angles at the Al atom of 118.80° and 118.35° for H_3SiAlH and H_3CAlH, respectively. Characteristic ν_a and δ_a IR frequencies for the SiH_3 and CH_3 groups, and bound AlH ν_s modes for both molecules are in agreement with accepted organic and inorganic compilations.[13,14] Reductive-elimination by broad band photolysis (520 nm, for H_3SiAlH, cf. 550 nm for H_3CAlH[7]) manifests itself in each of the spectroscopies employed showing photoreversibility to be inherent to both systems.

The important differences in electronic and bonding architecture between the two molecules are most pronounced in the EPR (observed and simulated spectra shown in Figure 3 for H_3SiAlH)

(5) Schubert, U.; Müller, J.; Alt, H. G. *Organometallics* **1987**, *6*, 469.
(6) Calculated via the method of Morton, J. R.; Preston, K. F. *J. Magn. Reson.* **1978**, *30*, 577.
(7) Parnis, J. M.; Ozin, G. A. *J. Phys. Chem.* **1988**, accepted for publication.
(8) Calculated from Al-hyperfine data in the following: Ammeter, J. H.; Schlosnagle, D. C. *J. Chem. Phys.* **1973**, *59*, 4784.
(9) 450-W Xe arc lamp (Osram) in an Oriel housing coupled to a 10-cm water-filled IR filter cell and an Oriel 7240 monochromator delivering 50–100 μW cm^{-2} at the sample.
(10) Parnis, J. M.; Ozin, G. A. *J. Am. Chem. Soc.* **1986**, *108*, 1699.
(11) Error in g values: ±0.001; error in A values: ±1 MHz. If the two lowest energy absorptions at 520, 305 nm are associated with the $^2A'(\pi) \rightarrow {}^2A'(\sigma)$ and $^2A'(\pi) \rightarrow {}^2A''(\pi)$ transitions of H_3SiAlH, this would imply to a first approximation that $g_1 \equiv g_z > g_e$ and $g_{2,3} \equiv g_{x,y} \simeq g_e$. $g_3 \equiv g_z$, $g_{1,2} \equiv g_{x,y} \simeq g_e$ based on the HOMO–LUMO $^2A'(\pi) \rightarrow {}^2A''(\pi)$ transition being associated with the 550-nm absorption of H_3CAlH.
(12) 6-31G** polarized basis-set: Hariharan, P. C.; Pople, J. A. *Chem. Phys. Lett.* **1972**, *16*, 217; *Theo. Chim. Acta.* **1973**, *28*, 213.
(13) Maslowsky, E., Jr. *Vibrational Spectra of Organometallic Compounds*; Wiley: New York, 1977.
(14) Nakamoto, K. *Infrared and Raman Spectra of Inorganic and Coordination Compounds*; 3rd ed.; Wiley: New York, 1978.

where increased ^{27}Al hyperfine splittings for H_3SiAlH results in a decrese in $\rho_{Al}(3p)$ to 62% from the 65% found in H_3CAlH and a concomitant decrease in proton superhyperfine interaction results in a drop of almost 7% (11% to 4.4%) in $\rho_H(1s)$. The $\rho_{Al}(3s)$ value of 20% remains the same. As mentioned before, such values are approximate.[6] Similar to the $Al(^2P)\{SiH_4\}$ complex the "missing" spin density is believed to reside on the Si atom of the SiH_3 group.

Acknowledgment. The generous financial support of the Natural Sciences and Engineering Research Council of Canada is greatly appreciated. The award of an Ontario Graduate Scholarship (M.A.L.) is deeply appreciated. Valuable computational assistance from Dr. Douglas McIntosh and Dr. Mike Peterson with various aspects of the EPR simulations and ab initio calculations are gratefully acknowledged.

A Concise Route to the Calicheamicin–Esperamicin Series: The Crystal Structure of a Core Subunit

Samuel J. Danishefsky,* Nathan B. Mantlo, and Dennis S. Yamashita

Department of Chemistry, Yale University New Haven, Connecticut 06511

Gayle Schulte

Yale University Instrumentation Center New Haven, Connecticut 06511

Received June 7, 1988

The goal of synthesizing the antitumor antibiotics esperamicin[1a] and calicheamicin[1b,2] is one which will engage the attention of synthetic organic chemists for some time. In addition to addressing the challenge intrinsically posed by these ornate systems, synthesis can be used to generate simpler variants which might mimic the quite extraordinary DNA cleaving properties of the drugs. The ultimate goal is the identification of compounds with greater margins of therapeutic usefulness.

A synthesis of a system containing an enediyne and a bridgehead olefin was accomplished by Schreiber and Kiessling.[3] A recent disclosure by Magnus and Carter provided the first simulation of the cycloaromatization chemistry of a synthetically derived enediyne, related to these antibiotics.[4] We have begun an investigation of the enediyne antibiotics with a view toward total synthesis and medicinal chemistry. *A direct thrust which leads in a few steps to an extensively functionalized core ensemble is now possible.* Moreover, the first crystallographically derived structural information on a prototype system has thus become accessible. Our results are described herein.

A central element of our strategy was the use of a benzenoid matrix to contain the functionality of the eventual cyclohexenone substructure of the natural products. At a strategic point, the system **1** would be exposed. The ketoaldehyde (Y undefined) would be merged with the previously described (*Z*)-dilithioenediyne **2**.[5] Crucial to success would be a productive choice of Y in structure **1**. The selection must harmonize the ease of

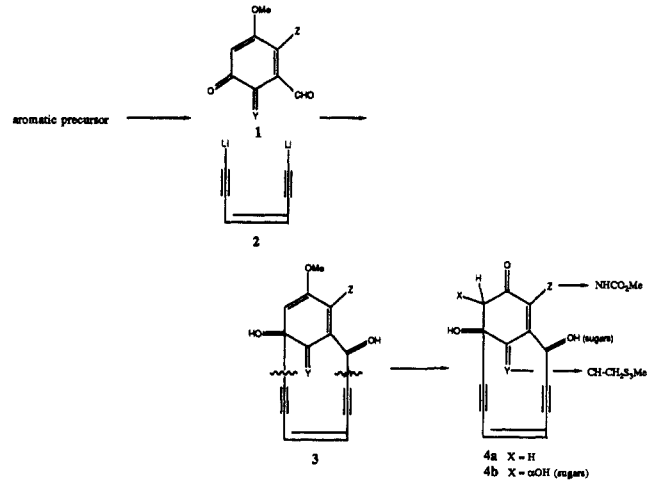

liberating **1** from the arene, the amenability of **1** to annulation via dilithium salt **2**, and the feasibility of installing the trisulfide moiety from Y.

The variation which we explored here is one where Y corresponds to a spiroepoxide, generated by the elegant chemistry of Adler and Becker.[6,7a,b] Compound **6** available by reduction ($LiAlH_4$) of **5**[8] when oxidized with sodium periodate in THF–H_2O

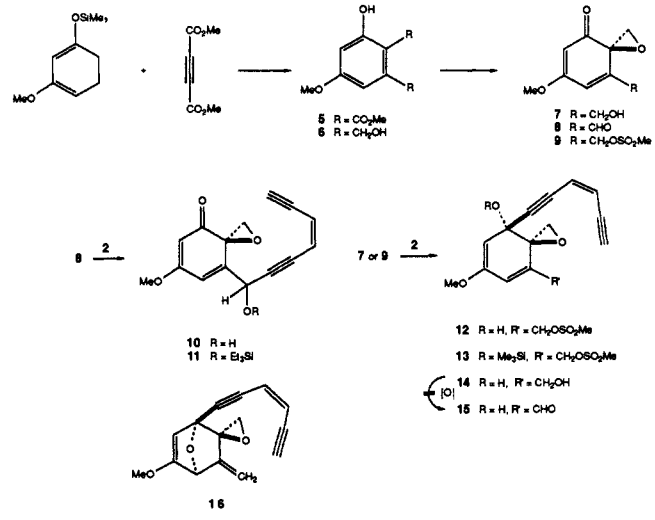

afforded **7** (65% overall yield). Reaction of **7** with the Dess–Martin periodinane gave a 70% yield of **8**.[9] Mesylation of **7** ($MeSO_2Cl$; Et_3N) afforded **9**. Seco systems **10**, **12**, and **14** were obtained in good yield by the monoaddition of dilithioenediyne **2** to compounds **8**, **9**, and **7**, respectively. Compounds **10** and **12** as well as their silylated derivatives **11** and **13** failed to undergo cyclization in the desired sense after treatment with lithium diisopropylamide. The product arising from **12** was the 7-oxanorbornene derivative **16**. *A remaining possibility to be screened was one in which cyclization would be attempted on an enediyne aldehyde of the type* ***15***. However, we were unable to reach this compound by oxidation of **14**.

Success was achieved by an adaptation of the Comins concept of in situ aldehyde protection.[10] Treatment of starting ketoaldehyde **8** in THF at −40 °C with lithio *N*-methylanilide generated what we surmised to be the corresponding lithio α-aminoalkoxide adduct. Administration of 2 equiv of dilithioenediyne

(1) (a) Golik, J.; Dubay, G.; Groenewold, G.; Kawaguchi, H.; Konishi, M.; Krishnan, B.; Ohkuma, H.; Saitoh, K.; Doyle, T. *J. Am. Chem. Soc.* **1987**, *109*, 3462. (b) Lee, M.; Dunne, T.; Siegel, M.; Chang, C.; Morton, G.; Borders, D. *J. Am. Chem. Soc.* **1987**, *109*, 3464, 3466. Zein, N.; Sihha, A. M.; McGahren, W. J.; Ellestad, G. A. *Science (Washington, D.C.)* **1988**, *240*, 1198.

(2) The revision in stereochemistry at C_{12} in calicheamicin from that initially published[1b] was suggested in a personal communication by Dr. M. Lee of the Lederle group.

(3) Schreiber, S. L.; Kiessling, L. L. *J. Am. Chem. Soc.* **1988**, *110*, 631.

(4) Magnus, P.; Carter, P. *J. Am. Chem. Soc.* **1988**, *110*, 1626.

(5) Danishefsky, S. J.; Yamashita, D. S.; Mantlo, N. B. *Tetrahedron Lett.*, in press.

(6) Adler, E.; Brasen, S.; Miyake, H. *Acta Chem. Scand.* **1971**, *35*, 2055. Becker, H.; Bremholt, T.; Adler, E. *Tetrahedron Lett.* **1972**, *41*, 4205.

(7) (a) Berchtold, G. A.; Sher, F. T. *J. Org. Chem.* **1977**, *42*, 2569. (b) Corey, E. J.; Dittami, J. P. *J. Am. Chem. Soc.* **1985**, *107*, 256. We note that the stereochemical course of the addition of dilithio salt **2** to compound **15** parallels that observed for a related process in this reference.

(8) McMurry, J.; Erion, M. *J. Am. Chem. Soc.* **1985**, *107*, 2712.

(9) Dess, D. B.; Martin, J. C. *J. Org. Chem.* **1983**, *48*, 4155.

(10) Comins, D. L.; Brown, J. D.; Mantlo, N. B. *Tetrahedron Lett.* **1982**, *23*, 3979. Comins, D. L.; Brown, J. D. *J. Org. Chem.* **1984**, *44*, 1078.

0002-7863/88/1510-6890$01.50/0